14. S.E. Battersby, R.F. Cochrane, and A.M. Mullis: *J. Mater. Sci.*, 1999, vol. 34, pp. 2049-56.
15. D. Li, K. Eckler, and D.M. Herlach: *Europhys. Lett.*, 1995, vol. 32, pp. 223-27.
16. D. Li, K. Eckler, and D.M. Herlach: *J. Cryst. Growth*, 1996, vol. 160, pp. 59-65.
17. D. Li, T. Volkmann, K. Eckler, and D.M. Herlach: *J. Cryst. Growth*, 1995, vol. 152, pp. 101-04.
18. C.F. Lau and H.W. Kui: *Acta Metall. Mater.*, 1991, vol. 39, pp. 323-27.
19. C.F. Lau and H.W. Kui: *Acta Metall. Mater.*, 1994, vol. 42, pp. 3811-16.

Approximate Models of Microsegregation with Coarsening

V. R. VOLLER and C. BECKERMANN

Microsegregation refers to the processes of solute rejection and redistribution at the scale of the dendrite arm spaces in the mushy region of a solidifying alloy. A representative geometry for a microsegregation analysis is the half-arm spacing in a "platelike" morphology (Figure 1). Models of microsegregation are based on a solute balance within this domain. A recent review by Kraft and Chen[1] covers the range of available models. Common assumptions used in modeling include a binary eutectic alloy; a fixed average composition, C_0; equilibrium at the solid-liquid interface; a constant partition coefficient $k < 1$; and a straight liquidus line in the phase diagram. Two key features of the solute balance that need to be included in a comprehensive model are the following.

(1) The mass diffusion of the solute. Typically, the solute diffusion in the liquid is rapid, and, at each instant in time, a uniform distribution of solute, $C_l(t)$, can be assumed. In the solid, however, diffusion is much slower and the solute balance needs to account for the so-called "back-diffusion" of solute into the solid.
(2) Changes in morphology. As solidification proceeds, the arm spacing will coarsen. If the overall solute balance is maintained in the half-arm domain, this feature will dilute the solute in the liquid.

One class of microsegregation models involves expressions that contain integrals. When coarsening is not accounted for and the solid growth is parabolic, Wang and Beckermann[2] obtain an integral expression that approximates the segregation ratio (C_1/C_0). At the opposite extreme, accounting for coarsening but neglecting back-diffusion, analytical expressions can also be obtained. In the case of a constant cooling rate, Mortensen[3] presents an analytical integral expression for the solid fraction, f, and Voller and Beckermann[4] present an analytical integral expression for the segregation ratio when solid growth is parabolic.

In recent work, Voller and Beckermann[4] show, analytically, that coarsening can be included in a microsegregation model by using the enhanced diffusion parameter

$$\alpha^+ = \frac{X_F^2}{X_0^2}\,\alpha + \frac{1}{X_0}\frac{dX_0}{d\tau}\frac{f^2}{m+1} \qquad [1]$$

In Eq. [1],

$$\alpha = \frac{Dt_F}{X_F^2} \qquad [2]$$

is the regular back-diffusion Fourier number, D is the diffusivity (m/s^2) in the solid, X_F is the length of the microsegregation domain at the conclusion of solidification—usually taken to be equal to half the final secondary arm spacing, and t_F is the local solidification time. The other terms in Eq. [1] are $X_0(\tau)$, the time-dependent length of the half arm space; f, the solid fraction in the arm space; $\tau = t/t_F$, the normalized time; and m, the order of the polynomial used to approximate the solid solute profile ($m = 2$ to 2.5[2,4]). The first term on the right-hand side of Eq. [1] accounts for the back-diffusion and the second term accounts for the coarsening-induced dilution of the liquid solute concentration. An important observation from Eq. [1] is that, in the absence of back-diffusion, the effect of coarsening on microsegregation is characterized by the diffusion parameter

$$\alpha^c = \frac{1}{X_0}\frac{dX_0}{d\tau}\frac{f^2}{m+1} \qquad [3]$$

Voller and Beckermann[4] show that, across a wide range of cooling conditions and for a coarsening law of the form $X_0 = \tau^{1/3}$, this term takes a constant value of $\alpha^c = 0.1$.

The objective of the current work is to use the result in Eqs. [2] and [3] to extend the current integral-based microsegregation models to arrive at general integral approximations that can take full account of both back-diffusion and coarsening.

The starting points for the general model development are the available analytical expressions for microsegregation in the presence of coarsening but absence of back-diffusion. Under this condition, when the solid growth is parabolic, Voller and Beckermann[4] obtain the exact microsegregation expression

$$\frac{C_1}{C_0} = \frac{2n\,(1-f)^{(1+2n)k-1}}{f^{2n}}\int_0^f \phi^{2n-1}\,(1-\phi)^{-(1+2n)k}\,d\phi \qquad [4]$$

where n is the exponent in a coarsening model of the form[5]

$$X_0 = \tau^n \qquad [5]$$

When the solidification is controlled by a constant cooling rate, Mortensen (Eq. [12] in Reference 3) obtains the exact expression

$$f = \frac{1+n}{1-k}\frac{C_1^{[1/(k-1)]}}{(C_1 - C_0)^n}\int_{C_0}^{C_1} \phi^{[k/(1-k)]}\,(\phi - C_0)^n\,d\phi \qquad [6]$$

The microsegregation models in Eqs. [4] and [6] are analytical but only applicable in the limit of coarsening alone (*i.e.*, there is no back-diffusion). A consequence of Eq. [3], however, is that coarsening can be considered to be a back-diffusion-like microsegregation process characterized by the enhanced diffusion term α^c. This suggests that, with an appropriate definition of the coarsening exponent n, Eqs. [4] and [6] could be applicable to back-diffusion–controlled microsegregation.

If the solidification is controlled by a parabolic growth of solid fraction

V.R. VOLLER, Professor, is with the Saint Anthony Falls Laboratory, Department of Civil Engineering, University of Minnesota, MN 55455-0116. C. BECKERMANN, Professor, is with the Department of Mechanical Engineering, University of Iowa, Iowa City, IA 52243.

Manuscript submitted April 5, 1999.

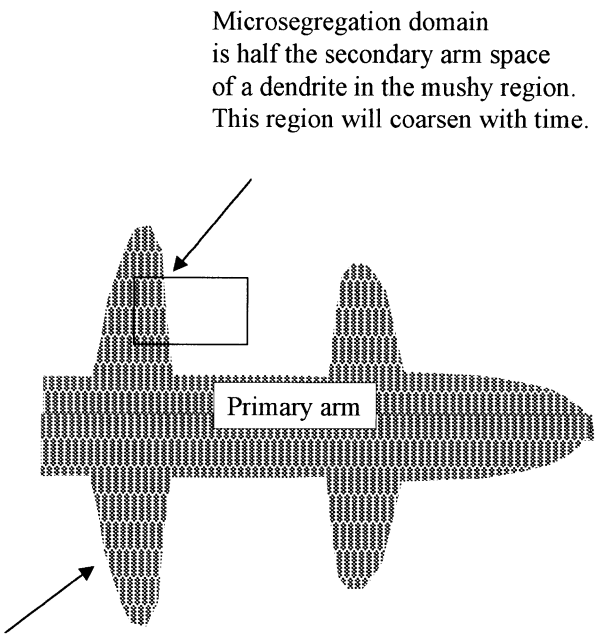

Fig. 1—Microsegregation domain is half-secondary dendrite arm space in a platelike morphology.

$$f = \tau^{1/2} \qquad [7]$$

then, with reference to Eq. [3],

$$\alpha^c = \frac{1}{X_0}\frac{dX_0}{d\tau}\frac{f^2}{m+1} = \frac{n}{m+1} \qquad [8]$$

This expression indicates that a coarsening-controlled microsegregation process, with a coarsening exponent,

$$n = (m+1)\alpha \qquad [9]$$

is equivalent to a back-diffusion–controlled microsegregation process characterized by the Fourier number α. Using Eq. [9] to replace n in Eq. [4] results in the following approximate relationship:

$$\frac{C_l}{C_0} = \frac{2(m+1)\alpha(1-f)^{((1+2(m+1)\alpha)k-1}}{f^{2(m+1)\alpha}} \int_0^f \phi^{2(m+1)\alpha-1}(1-\phi)^{-(1+2(m+1)\alpha)k} d\phi \qquad [10]$$

This expression is identical to the parabolic growth microsegregation model developed by Wang and Beckermann (Eq. [23] in Reference 2).

Although in a solidification controlled by a constant cooling rate the growth of the solid fraction is not parabolic, a parabolic growth may still be a reasonable "first cut" approximation. In this way, following from the arguments presented previously, the use of Eq. [9] to replace the coarsening exponent, n, in Eq. [6] will result in a back-diffusion only microsegregation model for a constant cooling rate. The result of this action is the approximate expression

$$f = \frac{1+(m+1)\alpha}{1-k}\frac{C_l^{[1/(k-1)]}}{(C_l - C_0)^{(m+1)\alpha}} \int_{C_0}^{C_l} \phi^{[k/(1-k)]}(\phi - C_0)^{(m+1)\alpha} d\phi \qquad [11]$$

Equations [10] and [11] are approximate models for microsegregation in the absence of coarsening. Equation [10], which has been presented in the literature previously,[2] is for the case when the solidification in the arm space is controlled by a parabolic growth. Equation [11] is for the case when the solidification is controlled by a constant cooling rate; this expression has not been previously presented. Taking guidance from the main result of Voller and Beckermann,[4] (Eq. [2]), these approximate models can be extended to the general case that includes both back-diffusion and coarsening by replacing the Fourier number, α, by the diffusion parameter

$$\alpha^+ = \frac{X_f^2}{X_0^2}\alpha + \frac{n}{m+1} \qquad [12]$$

In this way, the general version of the parabolic growth model, obtained from Eq. [10], is

$$\frac{C_l}{C_0} = (2A\alpha + 2n)\frac{(1-f)^{(1+2A\alpha+2n)k-1}}{f^{2A\alpha+2n}} \int_0^f \phi^{2A\alpha+2n-1}(1-\phi)^{-(1+2A\alpha+2n)k} d\phi \qquad [13]$$

where $A = (m+1)[X_F/X_0]^2$. Because the time-averaged behavior of the term $[X_F/X_0]^2$ is not known analytically, the parameter A is determined subsequently through a comparison with a full numerical solution of the microsegregation problem. In the limit of no coarsening ($n = 0$), Eq. [13] reduces to the model proposed by Wang and Beckermann,[2] and in the limit of coarsening alone ($\alpha = 0$), it reduces to the analytical model presented by Voller and Beckermann.[4] Integration by parts leads to the alternative form of Eq. [13]:

$$\frac{C_l}{C_0} = \frac{(1-f)^{(1+2A\alpha+2n)k-1}}{f^{2A\alpha+2n}} [f^{(2A\alpha+2n)}(1-f)^{-(1+2A\alpha+2n)k} - \int_0^f k(1+2A\alpha+2n)\phi^{2A\alpha+2n}(1-\phi)^{-(1+2A\alpha+2n)k-1} d\phi] \qquad [14]$$

This form is more suitable when the Fourier number, α, is small. For example, in the limit of $\alpha \to 0$ and $n = 0$, the Scheil equation[2]

$$\frac{C_l}{C_0} = (1-f)^{k-1} \qquad [15]$$

follows immediately from Eq. [14].

The general version of the constant cooling model, obtained by substituting Eq. [12] into Eq. [11] is

$$f = \frac{1+B\alpha+n}{1-k}\frac{C_l^{[1/(k-1)]}}{(C_l - C_0)^{B\alpha+n}} \int_{C_0}^{C_l} \phi^{[k/(1-k)]}(\phi - C_0)^{B\alpha+n} d\phi \qquad [16]$$

where B accounts for the time-averaged behavior of the product $(m + 1)[X_F/X_0]^2$. Note, in the limit of $\alpha = 0$, this equation matches the analytical model presented by Mortensen.[3]

Equation [13] or [14] and Eq. [16] are the key results in this article. For a given solidification path (parabolic growth or constant cooling), these models can be used to determine the progress of the complete microsegregation process including both back-diffusion and coarsening. This step, however, requires an evaluation of the integrals in Eqs. [13], [14], and [16] and the specification of the model parameters A and B.

For the parabolic growth models, the integrals in Eqs. [13] and [14] can be evaluated using a high-order numerical integration scheme. In this work, a 24-point Gaussian quadrature is used. If the Fourier number is small ($\alpha < 0.2$), then Eq. [14] should be evaluated for microsegregation predictions. If the Fourier number is large ($\alpha > 1$), then Eq. [13] should be evaluated. Practice shows that, when the Fourier number is small or large, a single application of the 24-point Gauss in the integration range $[0, f]$ is not of sufficient accuracy. In these cases, it is recommended that the integration domain be segmented (segments usually works well) with a 24-point Gauss applied in each segment. In terms of finding the parameter A, a crude fitting exercise (discussed subsequently) indicates that setting $A = 4.5$ works well across a wide range of conditions. Fortran programs for the evaluation of Eq. [13], parbig.for, and Eq. [14], parsmall.for, can be found on the web site http://www.ce.umn.edu/voller/voller__research/

The integral in the constant cooling model, Eq. [16], can also be evaluated with a single application of a 24-point Gaussian quatrature in the interval $[C_0, C_l]$. Further, setting the parameter $B = 3.8$ works well across a wide range of conditions. A Fortran program for the evaluation of Eq. [16], conapp.for, can be found on the web site http://www.ce.umn.edu/voller/voller__research/

The proposed models, Eq. [13] or [14] and Eq. [16], are tested by comparing their predictive performance with complete numerical models of microsegregation. These numerical models, which include both parabolic growth (parb.for) and constant cooling rate (const.for) versions, are fully reported elsewhere.[6] Appropriate Fortran 77 codes are available on the web site http://www.ce.umn.edu/voller/voller__research/

The predictive measure used for comparison will be the fraction of eutectic formed. The nominal concentration of the alloy is $C_0 = 1$ and the eutectic liquid concentration is $C_{eut} = 5$. Interest will focus on the variations of eutectic fraction with Fourier number, α, and partition coefficient, k. In all cases, a standard coarsening exponent of $n = 1/3$ will be used. [5] Note, when using the parabolic growth models, iterations need to be used to find the eutectic fraction.

Figure 2 compares eutectic predictions from the parabolic growth, Eq. [13] or [14], with predictions obtained from the full numerical model. For practical values of the partition coefficient, k, agreement between the approximate and numerical solutions, over a wide range of Fourier numbers, is very close. As a reference, eutectic predictions obtained when coarsening is absent ($n = 0$) and $k = 0.2$ are added to the figure. These results indicate the effect of coarsening

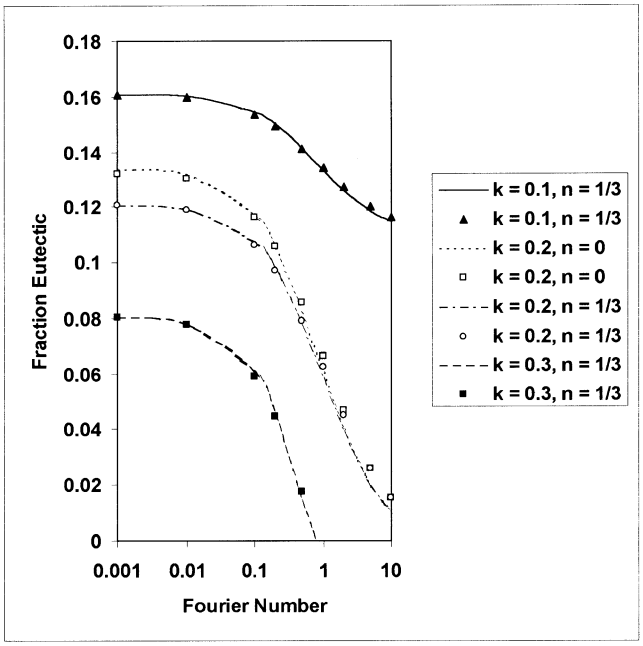

Fig. 2—Predicted eutectic fractions obtained with parabolic growth models. The continuous lines are the approximate model predictions; the points are numerical predictions.

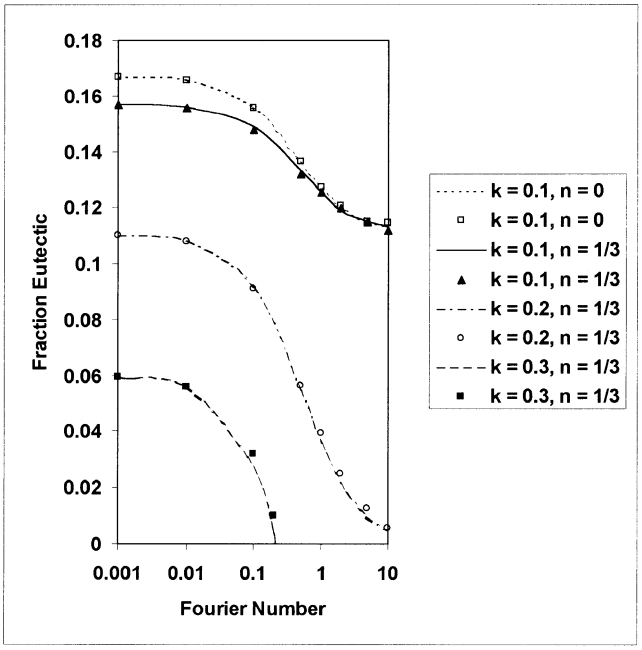

Fig. 3—Predicted eutectic fractions obtained with constant cooling models. The continuous lines are the approximate model predictions; the points are numerical predictions.

and provide a visual reference for the relative accuracy of the approximate expressions.

A similar comparison to those shown in Figure 2, but for the constant cooling model (Eq. [16]), is shown in Figure 3. Once again the comparison between the approximate and full numerical models is excellent.

A potential weak feature of the proposed models could be the choice of the fitting parameters A, in Eq. [13] or Eq.

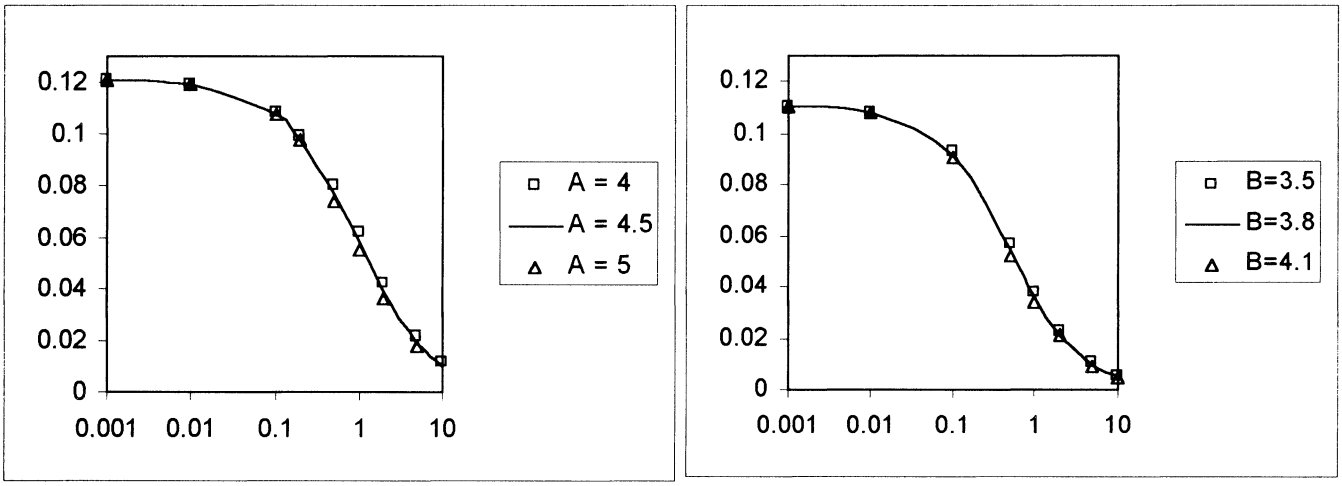

(*a*) (*b*)

Fig. 4—The effect of the fitting parameters *A* and *B*: (*a*) *A* in the parabolic growth model and (*b*) *B* in the constant cooling model.

[14], and *B*, in Eq. [16]. The reason that the optimum choice of these values is not the same ($A = 4.5$ and $B = 3.8$) indicates the fact that the assumption of a parabolic solid growth for the constant cooling case is reasonable but not exact. Eutectic predictions, however, are reasonably insensitive to the choices of *A* and *B*. Figure 4 compares predictions obtained with the proposed models in which the parameters *A* and *B* have been increased and decreased by ~10 pct. The results in this figure indicate very little change in the predictive ability of the approximate models when nonoptimum values of *A* and *B* are used and also suggest that a universal value of $A = B = 4$ would be appropriate for both models.

Exact integral expressions for microsegregation in a coarsening microstructure in the absence of back-diffusion have been reported in the literature.[3,4] Recent work by Voller and Beckermann[4] indicates that coarsening can be modeled in a standard microsegregation model as a back-diffusion process characterized by an enhanced diffusion parameter α^c (Eq. [3]). This result has been used to extend the analytical coarsening microsegregation models to approximate expressions that account for both coarsening and back-diffusion. The resulting integral expressions, one for a solidification controlled by a parabolic growth of solid (Eq. [13] or Eq. [14]) and one for a solidification controlled by a constant cooling rate (Eq. [16]), default to the appropriate limiting cases. In addition, across a wide range of practical conditions, predictions obtained with the approximate models compare closely with results from numerical models.

One of the authors (CB) gratefully acknowledges partial support provided by the National Science Foundation under Grant No. CTS-9501389.

REFERENCES

1. T. Kraft and Y.A. Chang: *J. Met.*, 1997, vol. 49, pp. 20-28.
2. C.Y. Wang and C. Beckermann: *Mater. Sci. Eng.*, 1993, vol. 171, pp. 199-211.
3. A. Mortensen: *Metall. Trans. A*, 1989, vol. 20A, pp. 247-53.
4. V.R. Voller and C. Beckermann: *Metall. Mater. Trans. A*, 1999, vol. 30A, pp. 2183-89.
5. D.H. Kirkwood: *Mater. Sci. Eng.*, 1985, vol. 73, pp. L1-L4.
6. V.R. Voller: *Int. J. Heat Mass Transfer*, in press, 1999.

Tensile Properties of Duplex Metal-Coated SiC Fiber and Titanium Alloy Matrix Composites

S.Q. GUO, Y. KAGAWA, A. FUKUSHIMA, and C. FUJIWARA

SiC(SCS-6) fiber-reinforced titanium alloy matrix composites have a great potential for high-temperature aerospace structural applications.[1,2,3] It is known that the interface reaction between the outermost SCS coating and Ti alloy matrix takes place during the fabrication process, and the formed reaction layer consists of a nonstoichiometric carbide (TiC_{1-x}) and silicides (Ti_xSi_y).[4,5,6] The reaction layer is brittle; however, this has only a slight effect on the quasi-static tensile strength.[7,8] On the other hand, the effect of the reaction layer cracking on the fatigue damage evolution is quite severe.[9,10,11] Such cracking under a cyclic fatigue loading condition leads to debonding of the SCS coating layer from the SiC fiber surface, which leads to a significant reduction in the fiber strength, because the debonding increases stress concentration at the SiC fiber surface, which originates from surface flaws of the fiber.[9,12] It was reported that the tensile strength of the SiC(SCS-6) fiber becomes about half of the original fiber strength after the debonding

S.Q. GUO, Postdoctoral Research Fellow, Japan Society for the Promotion of Science (JSPS), and Y. KAGAWA, Professor, are with the Institute of Industrial Science, The University of Tokyo, Tokyo 106-8558, Japan. A. FUKUSHIMA, Research Engineer, and C. FUJIWARA, Project Engineer, are with the Materials Research Section, Engineering Research Department, Nagoya Aerospace Systems, Mitsubishi Heavy Industries, Ltd., Nagoya 455-0024, Japan.

Manuscript submitted February 23, 1999.